

NASA Technical Memorandum 4779  
ARL Technical Report 1402

# Quasi-Static Viscoelasticity Loading Measurements of an Aircraft Tire

---

*Angela J. Mason and John A. Tanner*  
*Langley Research Center • Hampton, Virginia*

*Arthur R. Johnson*  
*Vehicle Technology Center*  
*U.S. Army Research Laboratory*  
*Langley Research Center • Hampton, Virginia*

Available electronically at the following URL address: <http://techreports.larc.nasa.gov/ltrs/ltrs.html>

Printed copies available from the following:

NASA Center for AeroSpace Information  
800 Elkridge Landing Road  
Linthicum Heights, MD 21090-2934  
(301) 621-0390

National Technical Information Service (NTIS)  
5285 Port Royal Road  
Springfield, VA 22161-2171  
(703) 487-4650

## Abstract

*Stair-step loading, cyclic loading, and long-term relaxation tests were performed on an aircraft tire to observe the quasi-static viscoelastic response of the tire. The data indicate that the tire continues to respond viscoelastically even after it has been softened by deformation. Load relaxation data from the stair-step test at the 15000-lb loading was fit to a monotonically decreasing Prony series.*

## Introduction

Aircraft tires are composite structures made of carbon-filled rubber, nylon cords, and steel wires. Under normal loading conditions, tires are subjected to large deformations with the constituents experiencing moderate strains. During aircraft ground operations and landings, the dynamic deformations of tires result in dissipative internal stresses. Tread friction and wear performance are affected, and heat is generated in the tire carcass. (See refs. 1 and 2.) Computational models that predict the dynamic responses of aircraft tires should address their viscous characteristics. The material properties needed in the viscoelastic constitutive models are determined by testing both coupons and full-size tires. (See refs. 3 to 9.)

The objective of this research activity is to expand the database on viscoelastic loading of full-size aircraft tires. An experimental program to establish the quasi-static mechanical response of the Space Shuttle orbiter nose-gear tire subjected to combined inflation pressure and vertical loading conditions is conducted. Stair-step loading, cyclic loading, and long-term relaxation tests are performed. Viscoelastic relaxation loads for the tire are approximated by least-squares fitting a Prony series to the load relaxation data. The least-squares fit is performed with the constraint that the coefficients of the exponential terms in the Prony series be positive (ref. 3). The Prony series model is intended for use in a separate effort in which viscoelastic finite element analyses are carried out to model the tire loading experiments.

## Test Apparatus

The aircraft tire used in this effort is a  $32 \times 8.8$ , type VII, bias-ply Shuttle nose-gear tire which has a 20-ply rated carcass and a maximum speed rating of 217 knots. The tread pattern consists of three circumferential grooves and the rated inflation pressure is 320 psi. The tire was inflated to 300 psi, which is consistent with previous tests performed on the tire. (See refs. 4, 10, and 11.) The rated operating load for the tire is 15 000 lb. A schematic of a typical bias-ply aircraft tire of similar construction is shown in figure 1.

The tire vibration stand (TVS) shown in figure 2 was used to perform the experiments. This equipment has

been used in a number of studies to determine tire damping characteristics (refs. 7 and 9) and tire footprints (refs. 10 and 11). The main structure of the TVS consists of two three-bay portal frames joined above by four beams (not shown in fig. 2) and along the floor by a thick plate. The tire rim is clamped between vertical supports to prevent rotation. A special feature of the TVS is the supporting of the test platen by four 5/8-in. wire rope cables. Each cable is suspended from a force-measuring load cell. The four load cells are connected through screw jacks to a frame with miter gears and worm-gear actuators. The frame is mechanically driven by an electric motor such that the four cables move simultaneously; thus, the platen is displaced in the vertical direction to load and unload the tire. A more detailed description of the TVS is found in reference 7.

A displacement transducer shown in figure 3 is mounted to the platen and affixed to the right adapter plate. This device measures the vertical displacements of the tire. The displacement transducer has a measuring span of  $\pm 10$  in. and a measurement accuracy of  $\pm 0.00657$  in. The four TVS load cells are connected in parallel, have a range of 0 to 120 000 lb, and have a measurement accuracy of  $\pm 134$  lb. A digital data acquisition system was used to collect the data at a recording rate of 5 samples/sec.

## Test Procedures

Three different experimental procedures were used. The first is referred to as "stair-step load relaxation testing"; the second, "cyclic testing"; and the third, "long-term relaxation testing." These procedures are described in the following paragraphs. In each test discussion, the targeted peak loads and time intervals are referenced. The targeted loads are 5000, 10 000, 15 000, 20 000, and 25 000 lb. Note, if the targeted peak load is 25 000 lb but the actual load reached is 25 300 lb, the discussion of the test procedure refers to the targeted load of 25 000 lb.

### Stair-Step Loading Test

The purpose of the stair-step loading test was to obtain a database for the time-dependent viscoelastic characteristics of the Shuttle nose-gear tire when subjected to incremental loading and unloading. Prior to starting this procedure the tire was inflated to 300 psi and

maintained in an unloaded condition for at least 24 hours to help ensure that the tire was fully relaxed in the pressurized state prior to starting the incremental loading tests. The desired time interval between loading increments was 190 sec. The technique used for the test consisted of loading and unloading the tire to a vertical load of 25 000 lb at 5000-lb increments. At each increasing load step, the vertical displacement was held constant and the load relaxation was recorded for 190 sec. A time of approximately 7 to 10 sec was required to increase (ramp up) the vertical load. After the peak load of 25 000 lb was reached, the process was reversed and the load was decreased to 0 lb in 5000-lb increments. Again, at each decreasing load step, the vertical displacement was held constant and the load rebound was recorded for 190 sec.

### **Cyclic Loading Test**

The second category of testing consisted of cyclically loading and unloading the Shuttle nose-gear tire. The primary focus of this test was to exercise and soften the tire. Tire hysteresis measurements were then made. The tire was again inflated to 300 psi and maintained in an unloaded condition for at least 24 hours prior to starting this procedure. The cyclic tests involved loading the tire from 0 lb to predetermined peak load and then unloading the tire as quickly as possible. There was no pause at the peak load during these tests and it took approximately 70 sec to complete one 25 000-lb cycle. The sequence of testing was initiated with ten 25 000-lb cycles followed by a series of tests wherein the tire was incrementally loaded and unloaded through the sequence of 5000, 10 000, 15 000, and 20 000 lb. The testing was conducted in one continuous operation.

### **Long-Term Relaxation Test**

The long-term relaxation test was performed to examine the relaxation behavior of the Shuttle nose-gear tire over long time intervals. Within 1 minute of the completion of either the stair-step test or the cyclic test, the tire was ramp loaded to a vertical load of 20 000 lb, the displacement was held constant, and the load relaxation was recorded for 900 sec. A variation of this test procedure included loading the tire to 25 000 lb and holding the displacement constant for 3200 sec. During these tests, the data acquisition system recorded continuously so that a complete time history could be obtained.

## **Experimental Results**

### **Stair-Step Loading Test**

Time histories of the tire vertical load and displacement are presented in figure 4. The figure shows time

histories of load and displacement for the stair-step test and a 20 000-lb, 900-sec, long-term relaxation test. The load time history (fig. 4(a)) and the displacement time history (fig. 4(b)) show the stair-step patterns associated with the test. The load time history exhibits relaxation during increasing load increments. This relaxation is indicated by load reduction over the 190-sec interval at each increasing load step. This effect is most pronounced at the higher load conditions. The load time history also exhibits load rebound during decreasing load increments of the test as indicated by a load increase over the 190-sec interval at each decreasing load step. This effect is most pronounced at the lower load conditions. The displacement plateau at each load step is flat; this indicates that the desired constant displacement test conditions were in fact achieved.

The load relaxation and rebound curves at the 15 000-lb loading (fig. 4) are enlarged and shown in figures 5 to 8. Figure 5 shows time histories of load and displacement as the load is increased from approximately 10 000 to 15 000 lb. The displacement time history (fig. 5(b)) indicates a constant displacement of 1.8 in. once the 15 000-lb level is reached. The load ramp and relaxation shown in the load time history in figure 5 is examined more closely in figure 6. The load ramp time history (fig. 6(a)) indicates that the load was increased from a starting point of about 9800 lb to a peak load of 15 400 lb in 7 sec. The load relaxation time history (fig. 6(b)) indicates a drop from 15 400 lb at the beginning of the 190-sec time interval to about 14 860 lb at the end of the time interval, a load relief of about 540 lb. Figure 7 shows time histories of load and displacement as the load is decreased from approximately 20 800 to 15 000 lb. The displacement time history (fig. 7(b)) indicates a constant displacement of 1.9 in. once the 15 000-lb load is reached. The load ramp and rebound shown in the load time history in figure 7 are examined more closely in figure 8. The load ramp time history (fig. 8(a)) indicates that the load was decreased from a starting point of about 20 800 lb to a minimum load of 14 730 lb in 7 sec. The load rebound time history (fig. 8(b)) indicates an increase from 14 730 lb at the beginning of the 190-sec time interval to about 15 030 lb at the end of the time interval. These load tests showed that there was a load rebound of about 300 lb.

Relaxation characteristics for each of the increasing load step cases are displayed in figure 9. This figure shows time-dependent load relaxation curves for each increasing load step from 5000 to 25 000 lb. The time-dependent load for each load step was derived by subtracting the minimum load from each point on the load relaxation time history for that load step and then adding 70 lb to the result. The data were initialized to 70 lb arbitrarily to compare the relaxation data. The Prony series

takes an infinite amount of time to relax to 0; therefore, the data were adjusted so that the Prony series least-squares fit algorithm could function properly. Other positive values selected did not significantly affect the data. For example, in the 15 000-lb load step relaxation data shown in figure 6, the time-dependent load curve for 15 000 lb in figure 9 is 610 lb at the beginning of the time interval and is reduced to 70 lb in 190 sec. The data in figure 9 indicate that the magnitudes of the rapidly decaying viscous load increments increased as the total load level increased.

Rebound characteristics for each of the decreasing load step cases are displayed in figure 10. The figure shows time-dependent load rebound curves for each decreasing load step from 20 000 to 5000 lb. The time-dependent load for each load step was derived by subtracting the minimum load from each point on the load rebound time history for that load step and then adding 70 lb to the result. Again 70 lb was selected arbitrarily. Thus for the 15 000-lb load step rebound data shown in figure 8, the time-dependent load, shown in figure 10, is 70 lb at the beginning of the time interval and increased to 370 lb in 190 sec. The data presented in figure 10 indicate that load rebound for the 20 000-lb load step is about 60 percent of the load rebound observed for the other decreasing load steps.

The time dependency of the tire load-deflection characteristics is further illustrated by displaying the incremental loading data versus displacement as given in figure 11. The 190-sec pauses allow the material to recover (relax) which produces a substantial hysteresis loop.

### Cyclic Loading Test

Figure 12 presents time histories of load and displacement for the cyclic loading test and a 25 000-lb, 900-sec, long-term relaxation test. The load time history (fig. 12(a)) and the displacement time history (fig. 12(b)) show a total of ten 25 000-lb loading and unloading cycles that were completed in about 700 sec. These cycles were followed by four cycles with peak loads that were changed in increments from 5000 lb to 20 000 lb over a period of about 150 sec. Finally, a 25 000-lb, 900-sec, long-term relaxation test completed this test sequence. The load time history exhibits load relaxation during the 25 000-lb relaxation test as indicated by load reduction over the 900-sec time interval. Again, the displacement plateau for the relaxation test is flat.

Load-deflection curves from the first, second, and tenth cyclic tests are presented in figure 13 to demonstrate the effect of conditioning on the hysteresis characteristics of the tire. Each test was conducted without any pauses; approximately 70 sec was required to complete

each cycle. The load-deflection curves are developed in a clockwise sense as indicated by the arrows in figure 13. The vertical load-deflection curves denote the commonly observed tire stiffening as the load and tire deformation become large. The initial cycle exhibits a well-defined hysteresis loop throughout most of the load range. Hysteresis losses for subsequent loading cycles were much less pronounced.

To better illustrate the effect of the cyclic loading history on the viscoelastic response of the tire, the thin hysteresis loops in figure 13 were least-squares fit to cubic polynomials. The plots of these polynomials are presented in figure 14. They demonstrate that the hysteresis loops are migrating to the right which is a measure of the viscoelastic softening of the tire. Immediately following the ten 0- to 25 000-lb load cycles, a series of four load cycle tests were conducted at loads ranging from 5000 to 20 000 lb. Load-deflection curves from these tests are presented in figure 15. These load-deflection curves are similar. They exhibit the low hysteresis characteristic associated with a work-conditioned tire, and each curve defines a similar nonlinear load-displacement response.

### Long-Term Relaxation Test

The long-term relaxation behavior of the tire is shown in figure 16. Time histories of viscoelastic load are presented for the 190-sec stair-step loading test at 20 000 lb (denoted by the solid line) and a 3200-sec, 20 000-lb relaxation test (denoted by the dashed line). Note that in figure 16, the curves were adjusted so that the maximum relaxation loads were equal at Time = 0. The 20 000-lb, 3200-sec relaxation test was initiated approximately 60 sec after the 900-sec relaxation test shown in figure 4. The data presented in figure 16 indicate that load relaxation characteristics for the stair-step test are similar to the characteristics for the first 190 sec of the long-term relaxation test. Furthermore, the long-term relaxation data demonstrate load relaxation throughout the entire 3200-sec time interval.

### Prony Series Relaxation Model

Constitutive models for viscoelastic materials are often expressed in their relaxation form. Consider a Maxwell material model (ref. 1), which is represented by a Prony series (also referred to as a "Dirichlet series"). The series is defined as follows:

$$f_v(t) = \sum_{i=1}^n A_i e^{-t/\tau_i}$$

where the coefficients  $A_i \geq 0$  (to ensure monotonic relaxation at all times) and  $\tau_i$  represents time constants. In the case of a constitutive model,  $A_i$  represents moduli. Here, we explore modeling the tire relaxation loads with a Prony series. The algorithm described in reference 3 was used to determine a Prony series for the 15 000-lb tire relaxation load shown in figure 6. A total of 24 time constants

$$\{\tau_i\}_{i=1}^{24} = \{10^{-9/4}, 10^{-2}, 10^{-7/4}, \dots, 10^{13/4}, 10^{7/2}\}$$

were considered and an optimal fit to the relaxation data was made with the constraint that  $A_i \geq 0$ . The magnitudes of the coefficients are shown in the top plot of figure 17, and the Prony series representation of the load relaxation is shown in the bottom plot of the figure. There were five nonzero coefficients in the resulting series which produced an excellent representation of the data.

### Concluding Remarks

Tests were conducted to determine the quasi-static viscoelastic characteristics of the Space Shuttle orbiter nose-gear tire. The following observations are noted:

The initial load cycle for a tire which has been unloaded for 24 hours exhibits a well-defined hysteresis loop. Hysteresis losses for subsequent loading cycles were much less pronounced.

The vertical load-deflection curves for the tire demonstrate a nonlinear stiffening behavior as the load is increased.

During the stair-step loading test, each successive increasing 5000-lb load increment resulted in a larger component of rapidly decaying load than that produced by the previous load increment. A similar pattern was not obtained for decreasing load increments.

The relaxation curves obtained in the stair-step loading test are similar to the load relaxation curve for the first 190 sec of the long-term relaxation test. Furthermore, the long-term relaxation test data demonstrated load relaxation throughout the entire 3200-sec time interval.

An optimization algorithm was used to least-squares fit relaxation data to a monotonically decreasing

Prony series. The Prony series approximation is in excellent agreement with the experimental data.

NASA Langley Research Center  
Hampton, VA 23681-2199  
May 20, 1997

### References

1. Clark, Samuel K., ed.: *Mechanics of Pneumatic Tires*. U.S. Dep. Transportation, 1981.
2. Futamura, S.: Effect of Material Properties on Tire Performance Characteristics—Part II: Tread Material. *Tire Sci. & Technol.*, vol. 18, no. 1, Jan.–Mar. 1990, pp. 2–12.
3. Johnson, A. R.; Quigley, C. J.; and Mead, J. L.: Large Strain Viscoelastic Constitutive Models for Rubber—Part I: Formulations. *Rubber Chem. & Technol.*, vol. 67, no. 5, Nov.–Dec. 1994, pp. 904–917.
4. Johnson, Arthur R.; Tanner, John A.; and Mason, Angela J.: A Kinetically Driven Anisotropic Viscoelastic Constitutive Model Applied to Tires. *Computational Modeling of Tires*, Ahmed K. Noor and John A. Tanner, eds., NASA CP-3306, 1995, pp. 39–51.
5. Kumar, M.; and Bert, C. W.: Experimental Characterization of Mechanical Behavior of Cord-Rubber Composites. *Tire Sci. & Technol.*, vol. 10, nos. 1–4, Jan.–Dec. 1982, pp. 37–54.
6. Quigley, Claudia J.; Mead, Joey; and Johnson, Arthur R.: Large Strain Viscoelastic Constitutive Models for Rubber—Part II: Determination of Material Constants. *Rubber Chem. & Technol.*, vol. 68, no. 2, May–June 1995, pp. 230–247.
7. Sleeper, R. K.; and Dreher, R. C.: *Tire Stiffness and Damping Determined From Static and Free-Vibration Tests*. NASA TP-1671, 1980.
8. Johnson, A. R.; Quigley, C. J.; Young, D. G.; and Danik, J. A.: Viscohyperelastic Modeling of Rubber Vulcanizates. *Tire Sci. & Technol.*, vol. 21, no. 3, July–Sept. 1993, pp. 179–200.
9. Davis, Pamela A.: *Quasi-Static and Dynamic Response Characteristics of F-4 Bias-Ply and Radial-Belted Main Gear Tires*. NASA TP-3586, 1997.
10. Howell, William E.; Perez, Sharon E.; and Vogler, William A.: *Static Footprint Local Forces, Areas, and Aspect Ratios for Three Type VII Aircraft Tires*. NASA TP-2983, 1991.
11. Tanner, John A.: *Computational Methods for Frictional Contact With Applications to the Space Shuttle Orbiter Nose-Gear Tire*. Ph.D. Thesis, George Washington Univ., Jan. 1993.

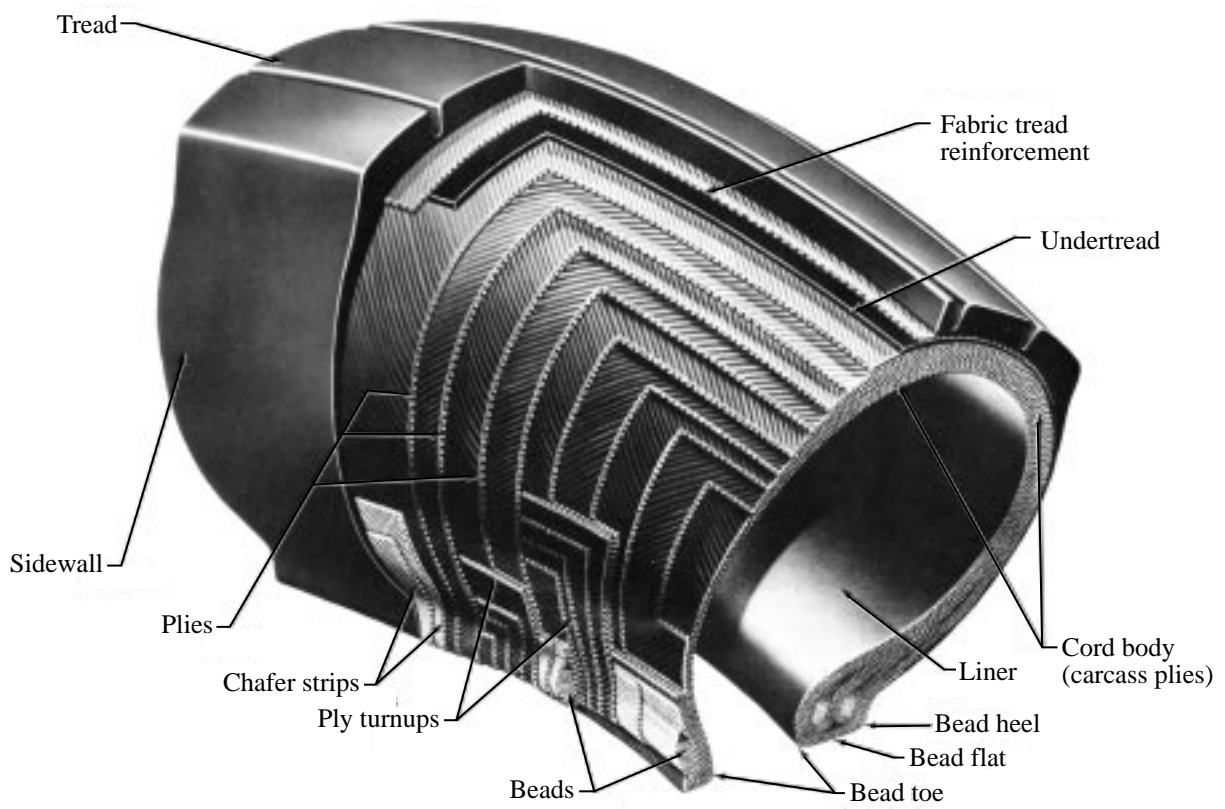


Figure 1. Aircraft tire construction.

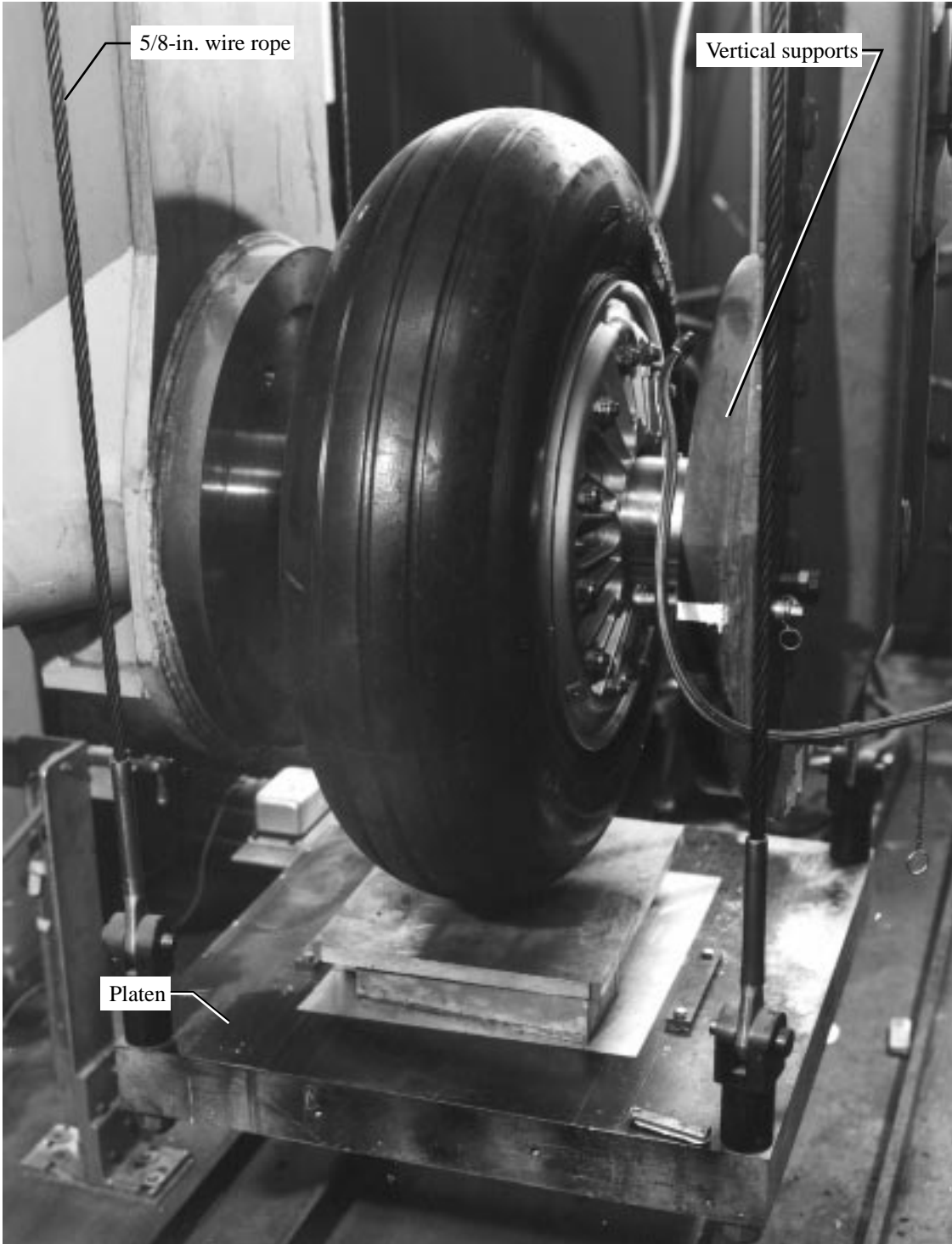


Figure 2. Tire vibration stand.

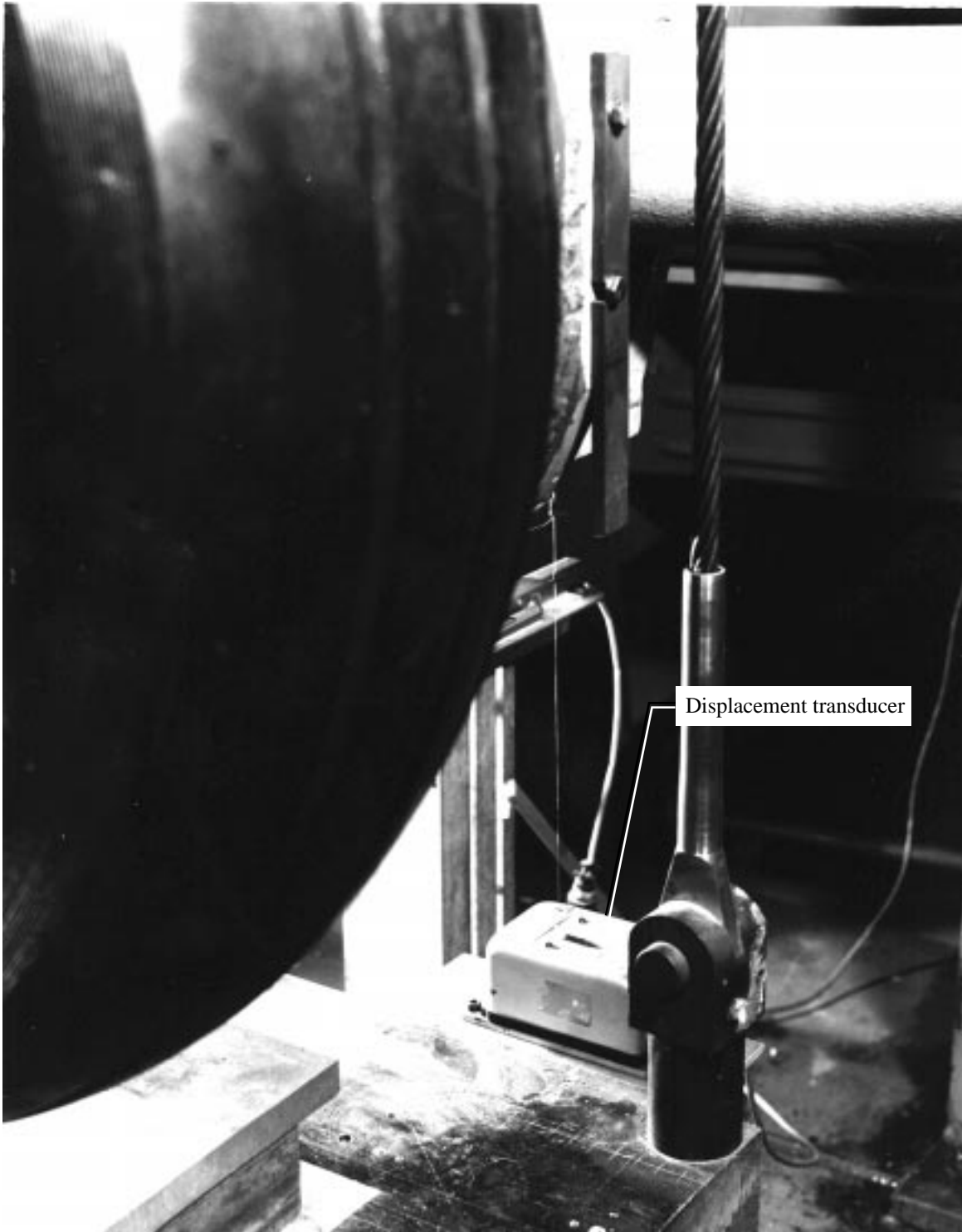
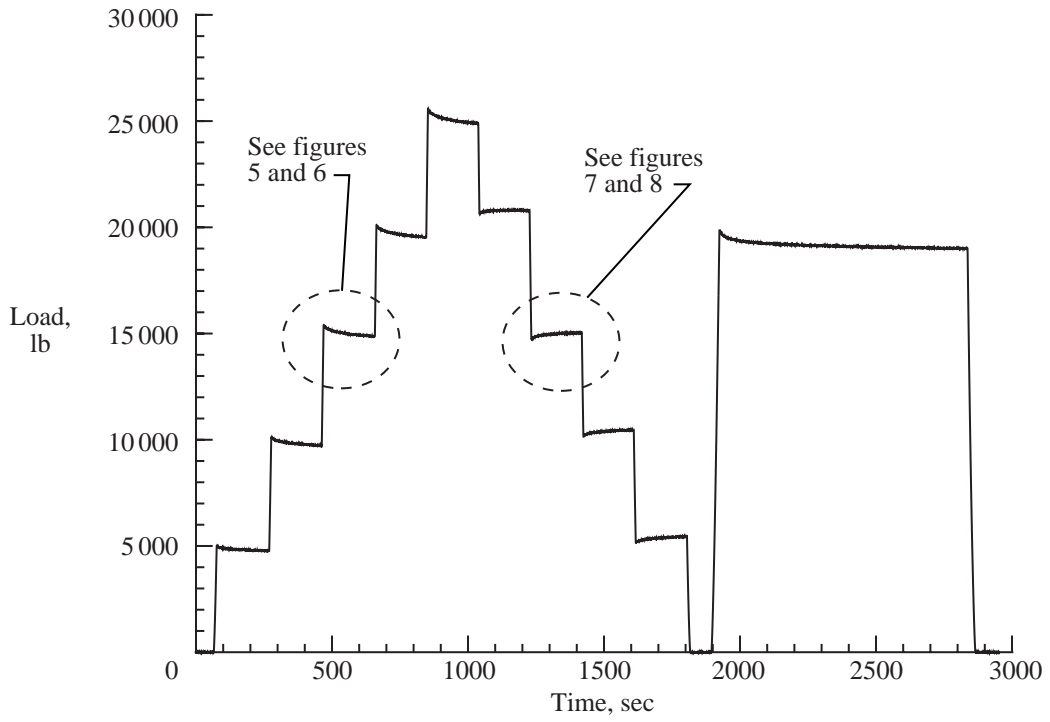
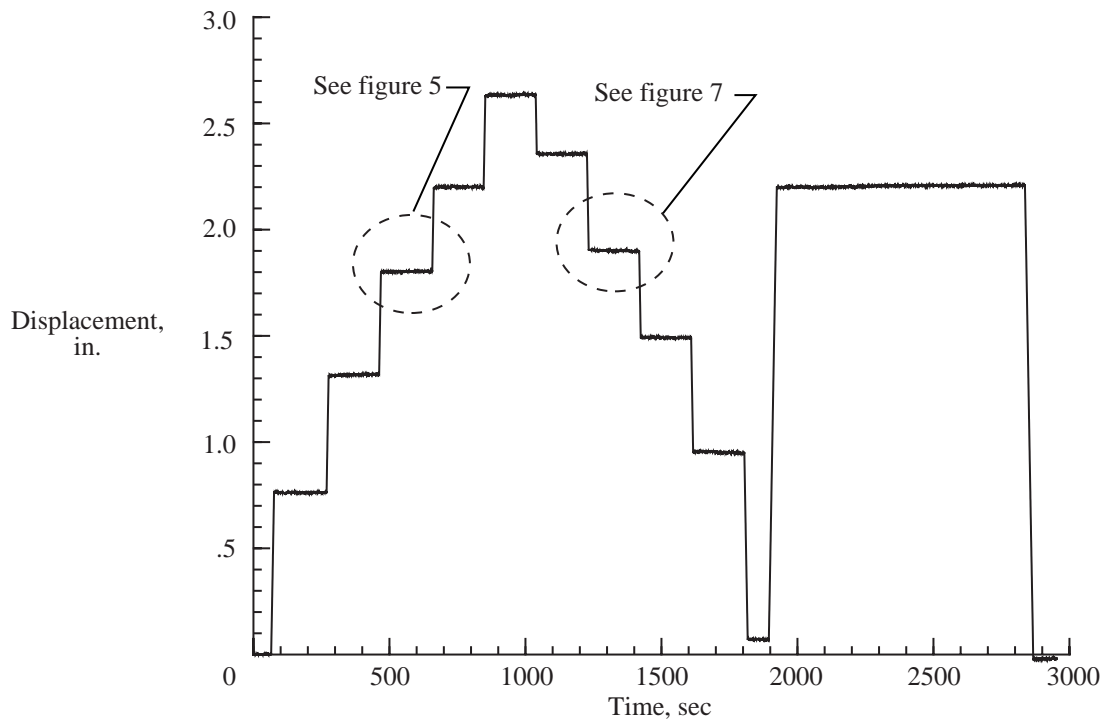


Figure 3. Displacement measurement device.

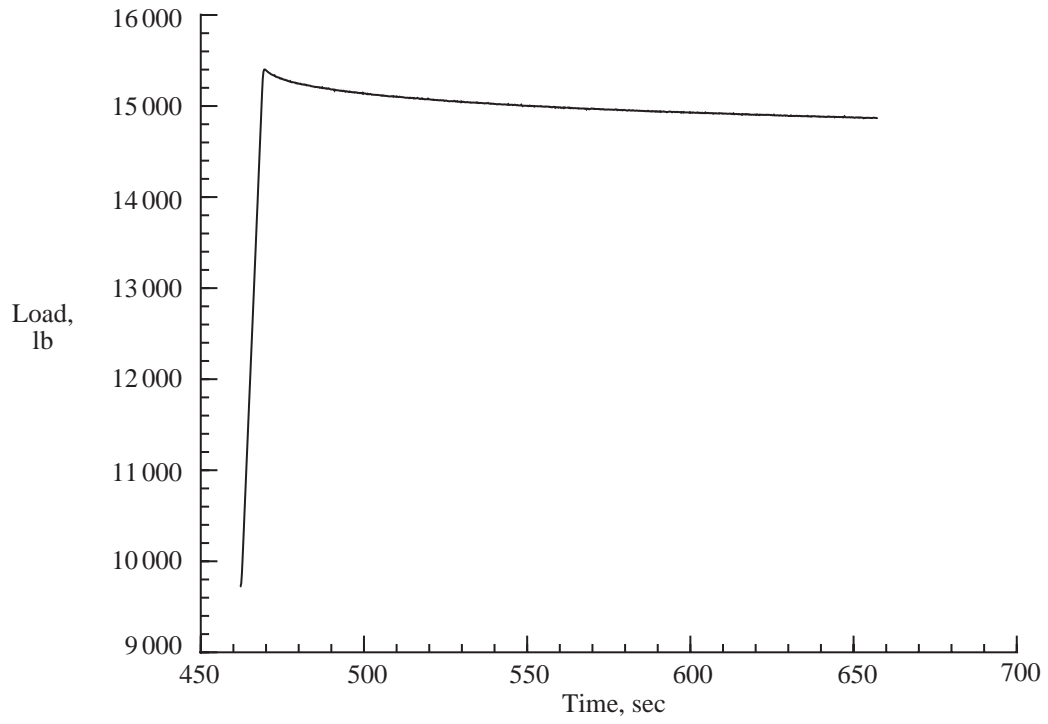


(a) Load.

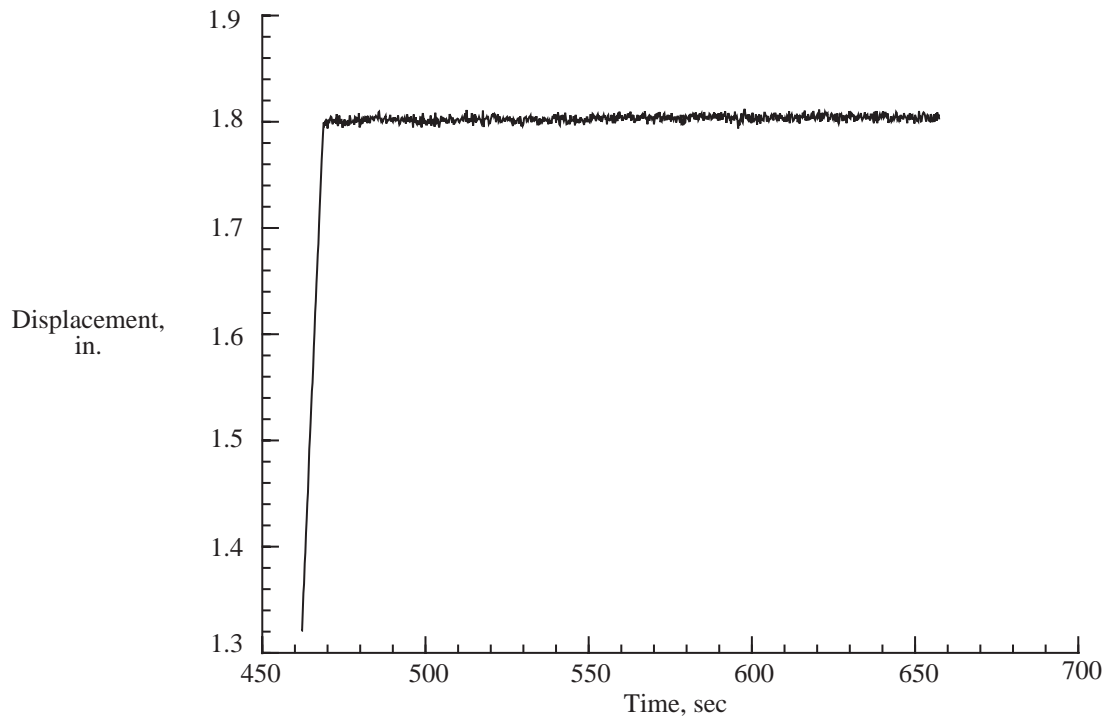


(b) Displacement.

Figure 4. Time histories of load and displacement for stair-step and long-term relaxation load tests.

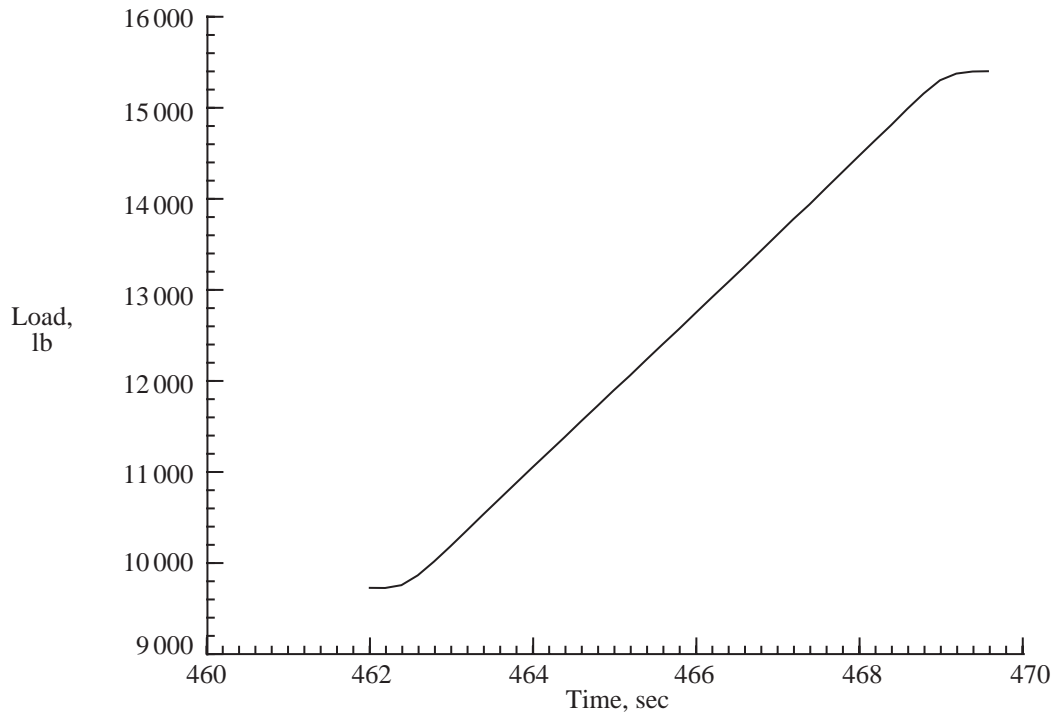


(a) Load.

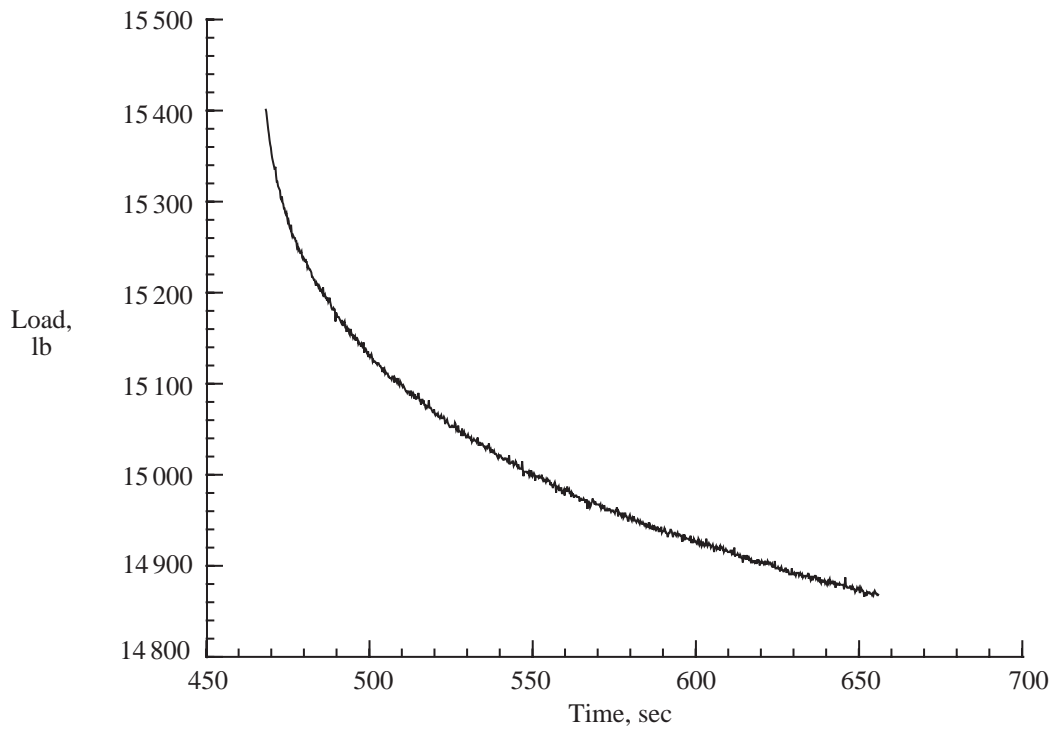


(b) Displacement.

Figure 5. Time histories of load and displacement for incremental loading from 10 000 to 15 000 lb.

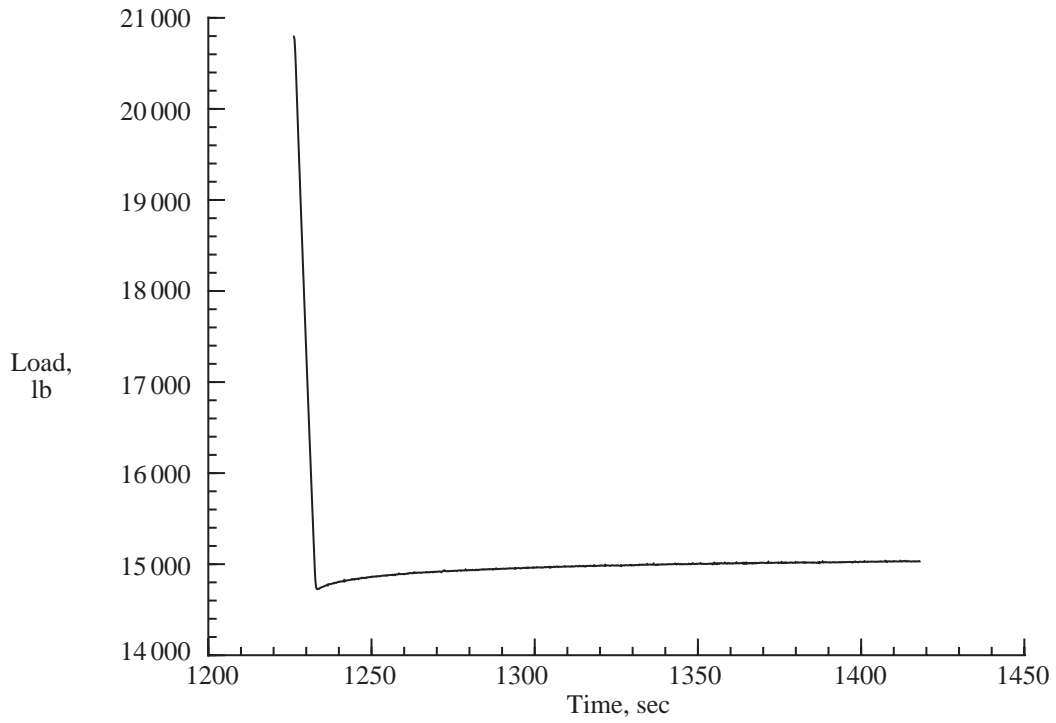


(a) Load ramp.

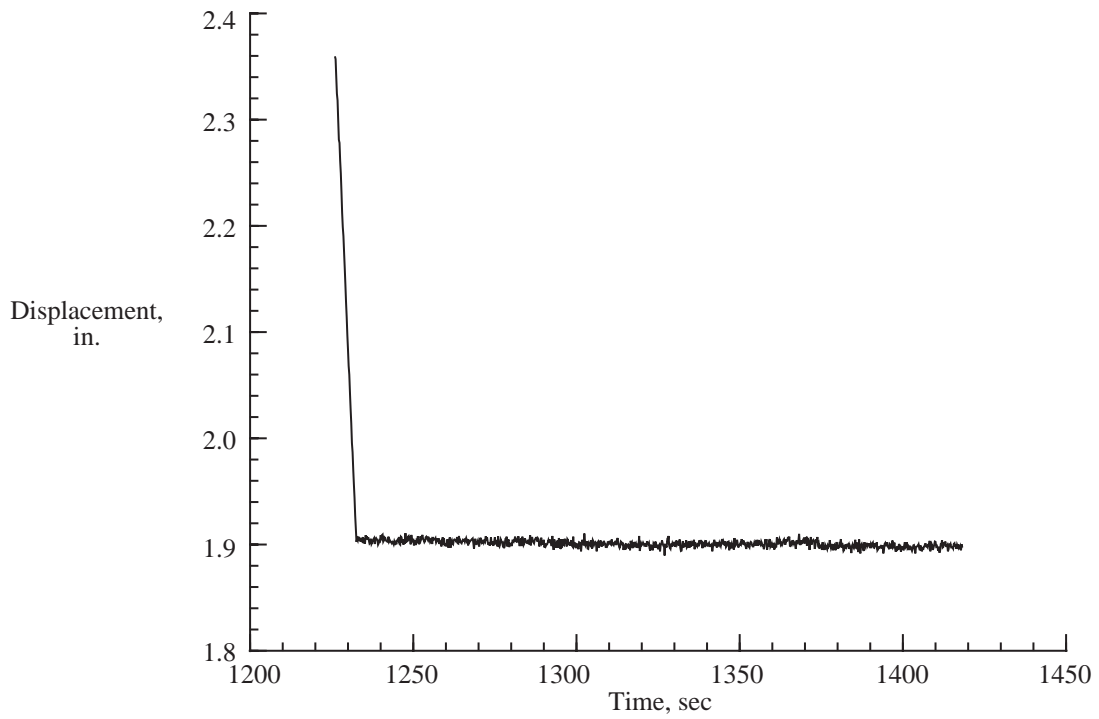


(b) Load relaxation.

Figure 6. Time histories of load ramp and load relaxation for incremental loading from 10 000 to 15 000 lb.

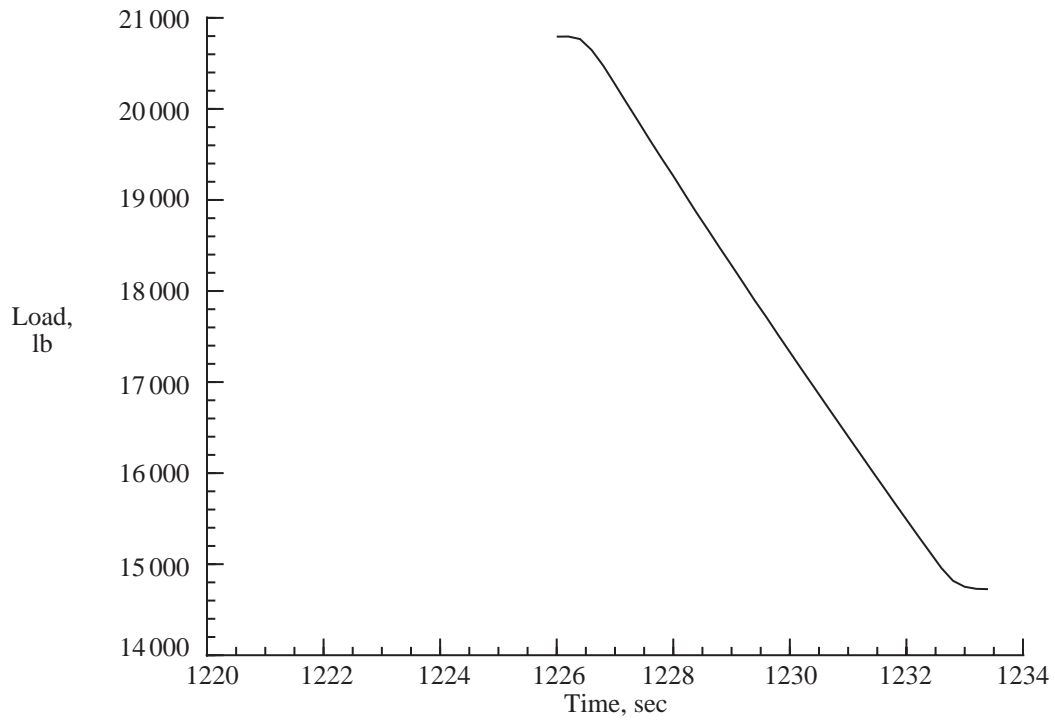


(a) Load.

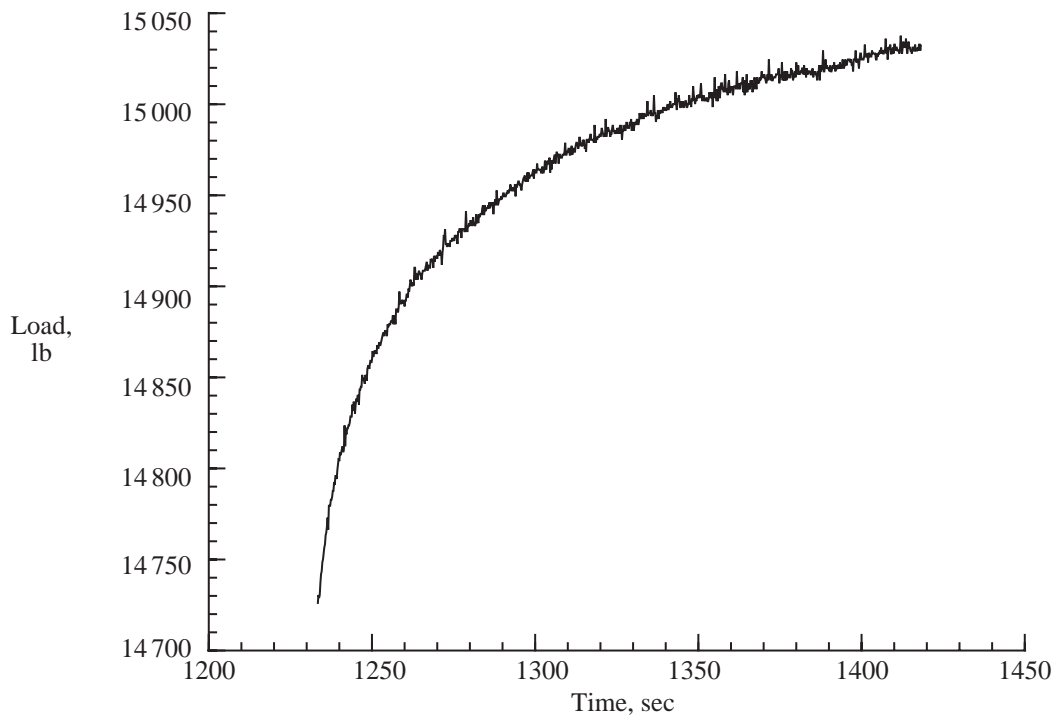


(b) Displacement.

Figure 7. Time histories of load and displacement for incremental loading from 20 000 to 15 000 lb.



(a) Load ramp.



(b) Load rebound.

Figure 8. Time histories of load ramp and load rebound for incremental loading from 20 000 to 15 000 lb.

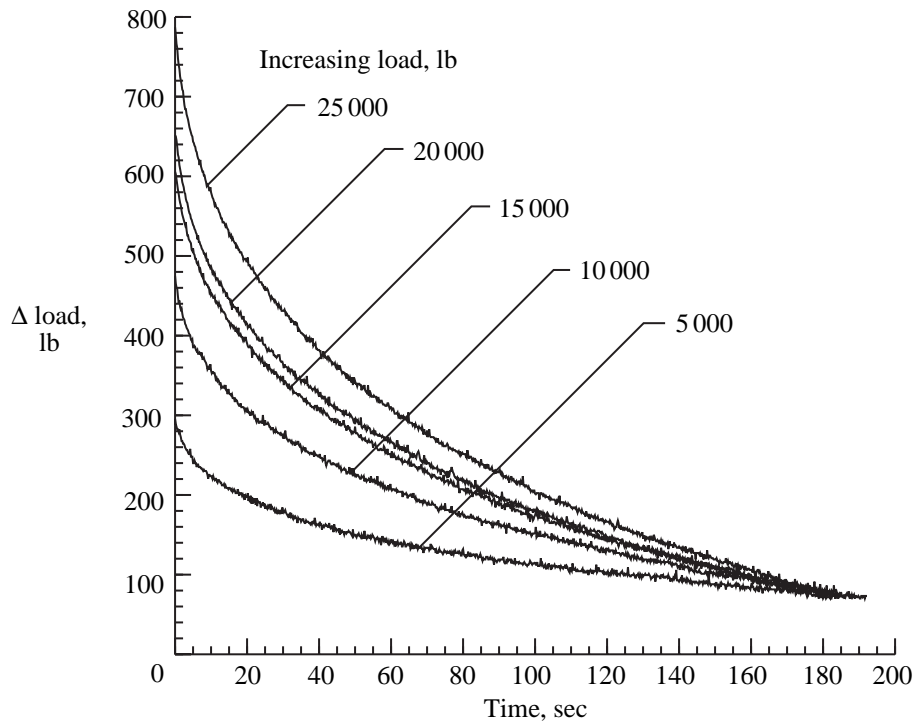


Figure 9. Stair-step test with increasing load viscoelastic results.

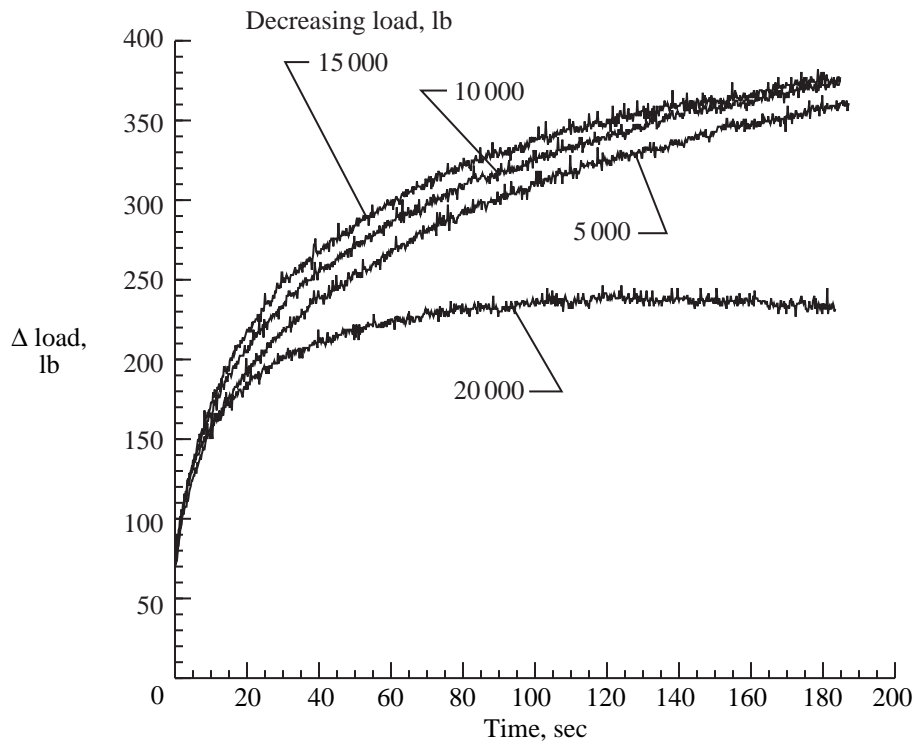


Figure 10. Stair-step test with decreasing load viscoelastic results.

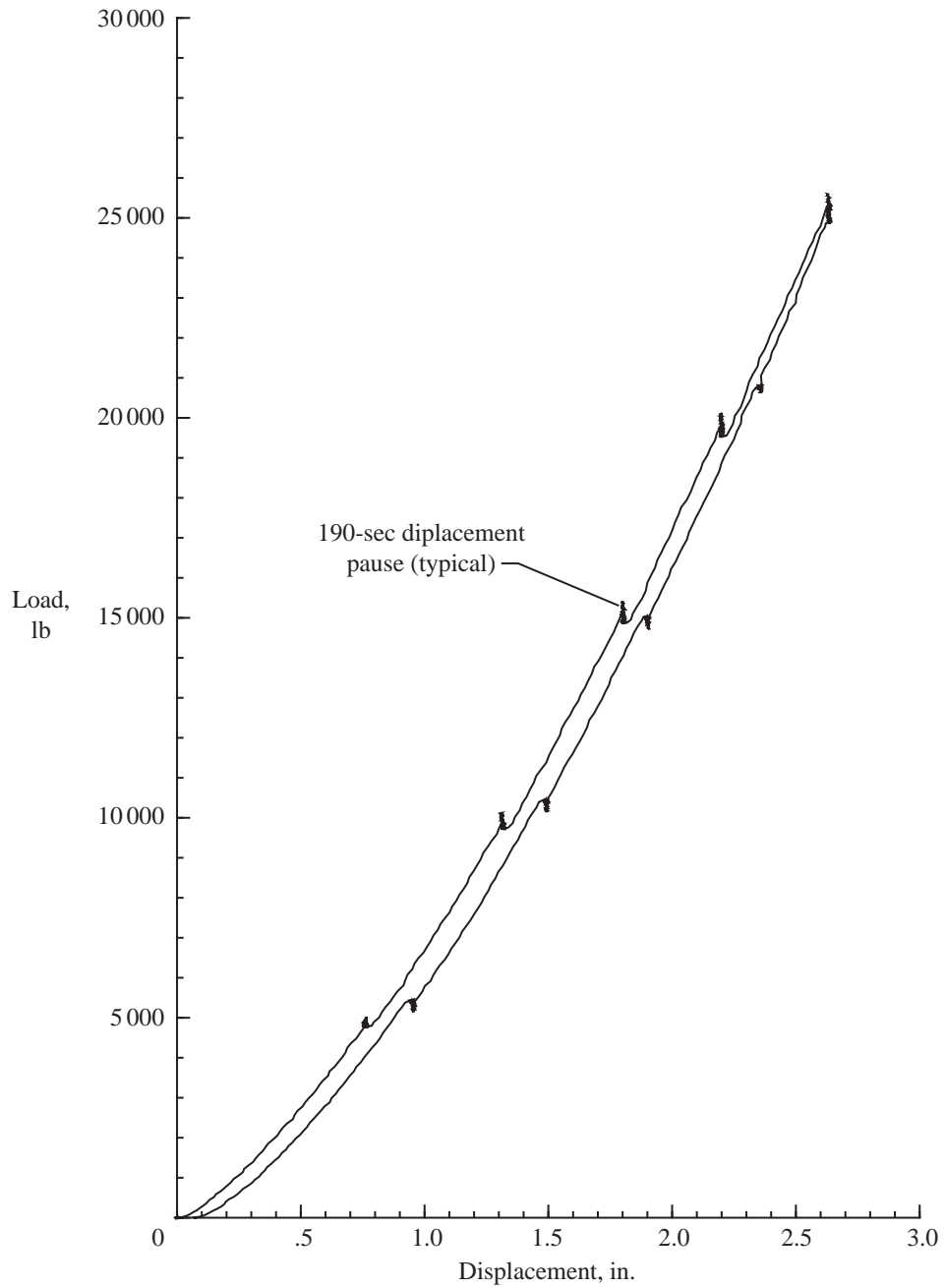
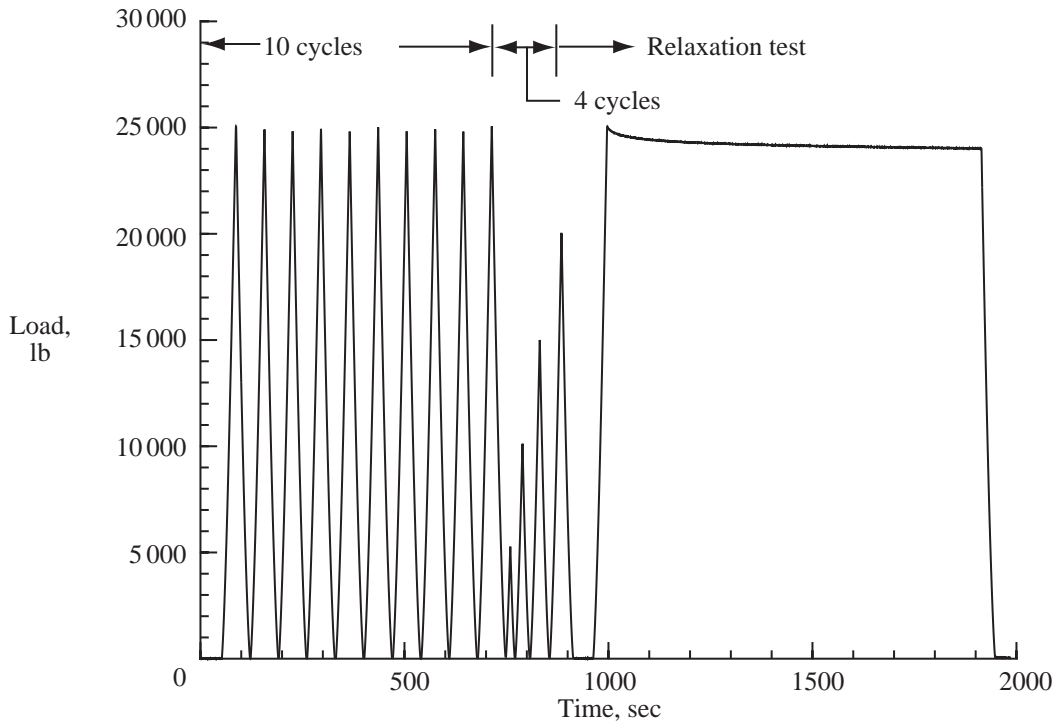
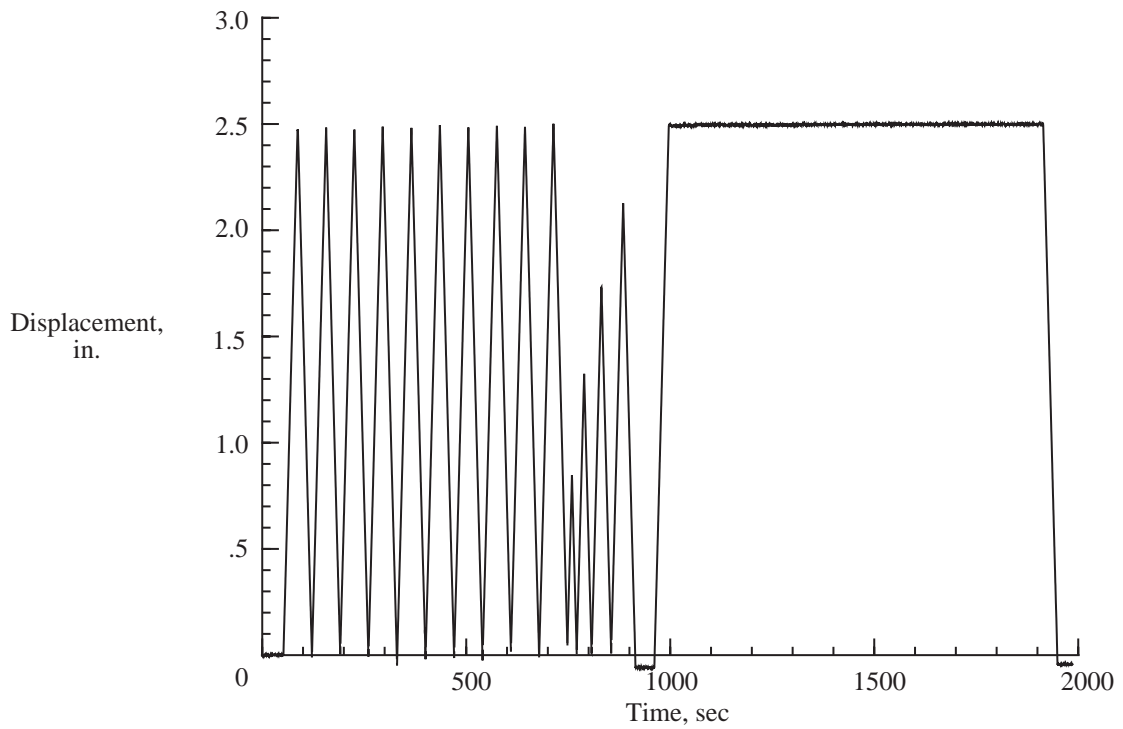


Figure 11. Load-deflection curve associated with stair-step test.



(a) Load.



(b) Displacement.

Figure 12. Time histories of load and displacement for cyclic loading and long-term relaxation load tests.

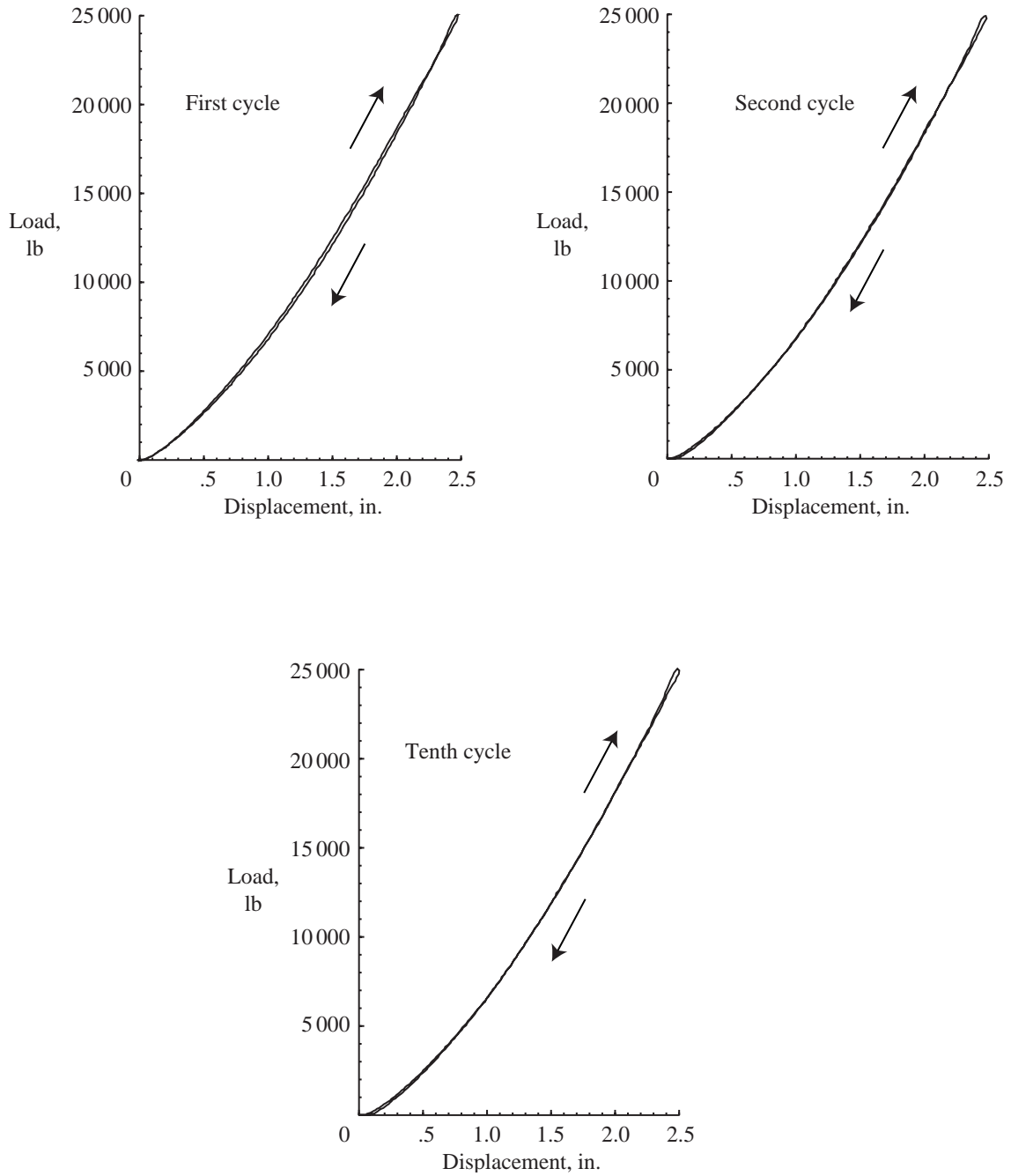


Figure 13. Typical load-deflection curves for cyclic loading test.

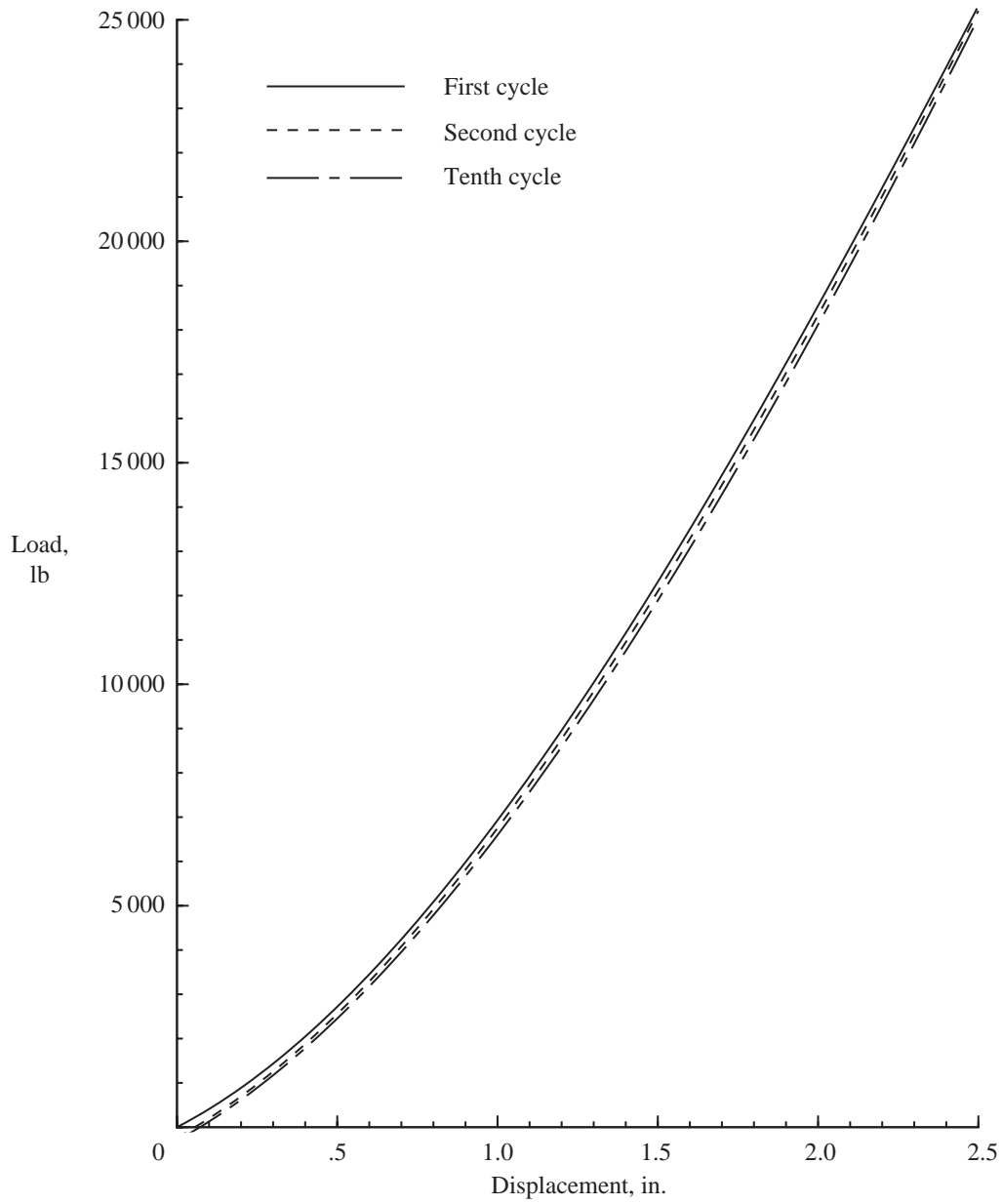


Figure 14. Least-squares approximation of hysteresis loops for cyclic loading test.

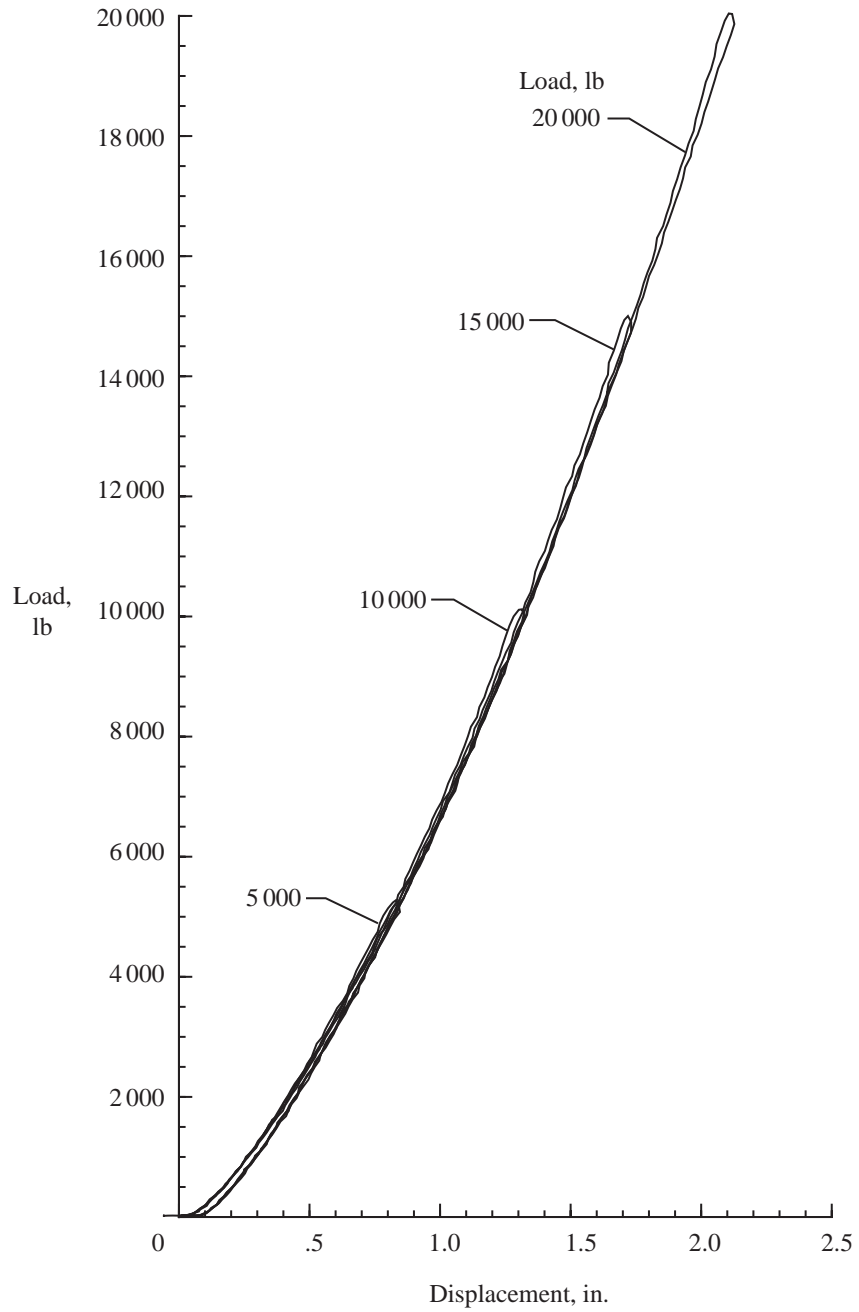


Figure 15. Hysteresis curves for loads from 5000 through 20 000 lb.

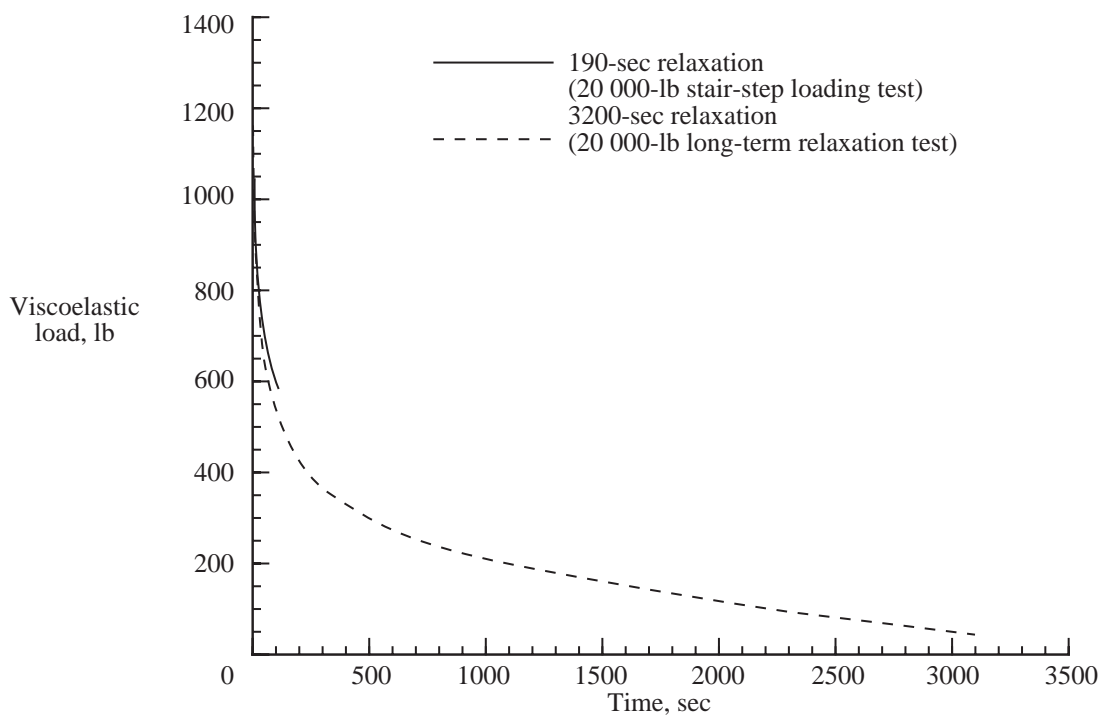


Figure 16. Long-term relaxation and stair-step tests results.

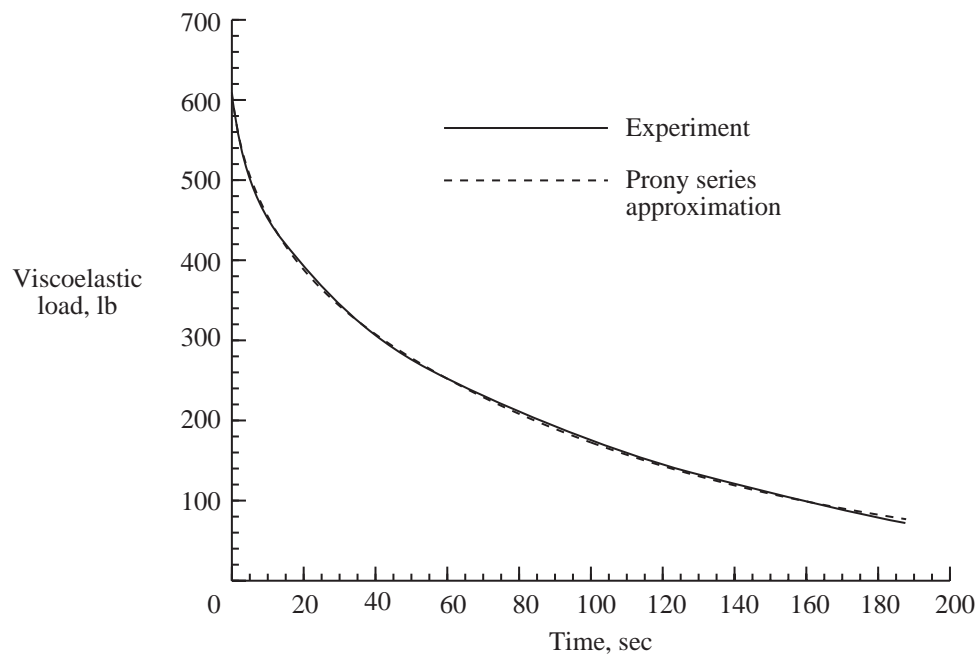
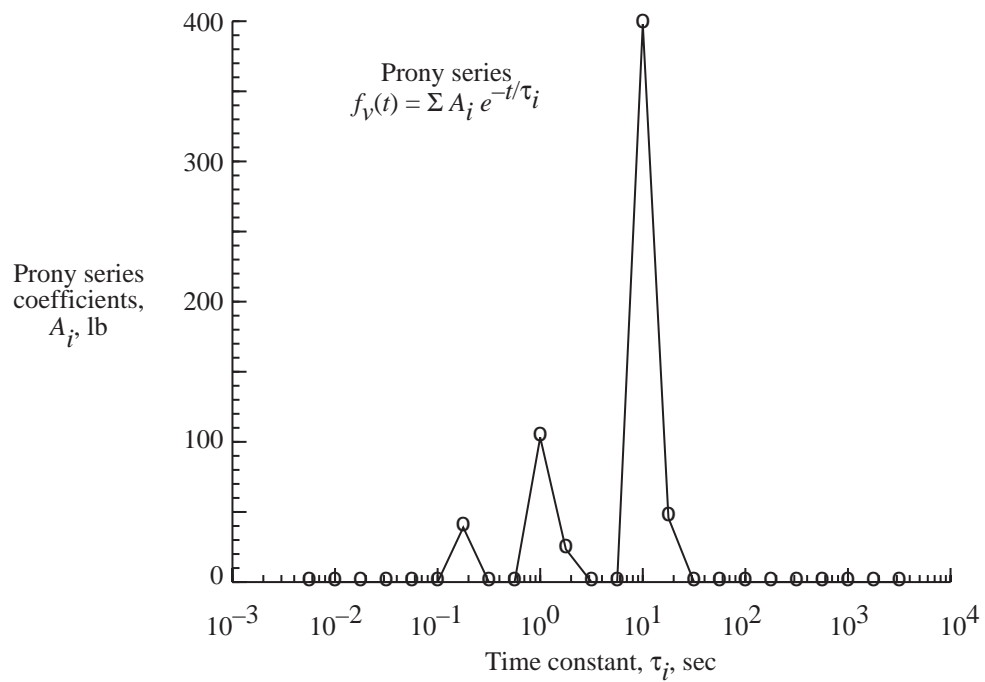


Figure 17. Prony series approximation of tire relaxation characteristics.



